A morganucodontan mammaliaform from the Upper Jurassic Morrison Formation, Utah, USA

BRIAN M. DAVIS, KAI R.K. JÄGER, GUILLERMO W. ROUGIER, KELLI TRUJILLO, and KEVIN CHAMBERLAIN

We describe two skull fragments of a new morganucodontan from the Cisco Mammal Quarry (Upper Jurassic Morrison Formation), preserving portions of the palate and snout in excellent 3D detail as well as the complete upper postcanine dentition. Morganucodontans are best known by isolated elements and relatively complete skulls of several species of *Morganucodon* from the Lower Jurassic of Wales and China; this group is fundamental to our understanding of the early evolution of mammals. *Cifellilestes ciscoensis* gen. et sp. nov. possesses derived features of the snout paired with plesiomorphic construction of the molars; the distal premolars are complex and there is an unusually low count (two) of strongly imbricated molars. This character combination expands craniodental variation for the group. We sampled mudstone from the Cisco Mammal Quarry for ash-fall zircon analysis and obtained a date of 151.50 ± 0.28 Ma. This dates the locality to the earliest Tithonian and slightly younger than other major dated mammal-bearing localities in the Morrison Formation. *Cifellilestes* represents one of the youngest members of this group and extends the record of morganucodontans in North America by more than 30 Ma. Morganucodontans are a rare component of Late Jurassic faunas but display surprising dental diversity through variations in a tooth count and cusp morphology of a deeply conserved, generalized mammalian tooth pattern, which was fully established in brasilodontid (non-mammalian) ancestors at least 80 my prior.

Key words: Mammalia, Morganucodonta, dentition, Jurassic, Morrison Formation.

Brian M. Davis [bm.davis@louisville.edu] and Guillermo W. Rougier [grougier@louisville.edu], Department of Anatomical Sciences and Neurobiology, University of Louisville School of Medicine, 511 S. Floyd St. Room 111, Louisville, KY, USA.
Kai R.K. Jäger [jaegerk@uni-bonn.de], Section of Palaeontology, Institute of Geosciences, Rheinische Friedrich-Wilhelms-Universität, Nussallee 8, 53115, Bonn, Germany.
Kelli Trujillo [kellitrujillo@me.com], Laramie County Community College, 1400 E College Dr, Cheyenne, WY, USA.
Kevin Chamberlain [kchamber@uwyo.edu], Department of Geology and Geophysics, University of Wyoming, 1000 E. University Ave., Dept. 3006, Laramie, WY, USA.

Introduction

Mammaliaformes is the clade containing the last common ancestor of Mammalia and Morganucodontidae plus all taxa in between (Rowe 1988), with a fossil record dating back to the Late Triassic (Kielan-Jaworowska et al. 2004, and references therein). Morganucodontans had a cosmopolitan distribution during the Late Triassic and Early Jurassic with records from the United Kingdom, continental Europe, China, United States, Africa, and India (see review in Debuysschere et al. 2015). The record of morganucodontans is considerably more sparse later in the Jurassic, with well-supported Bathonian records only from the UK (Freeman 1979; Butler

and Sigogneau-Russell 2016). The group persisted until the end of the Jurassic, with the youngest unambiguous record being a single upper molar from the Late Jurassic of Germany (Martin et al. 2019). A taxon referred to the Morganucodonta (a more inclusive clade containing morgancondontids and megazostrodontids, see Kielan-Jaworoska et al. 2004) has also been described from the earliest Cretaceous of England (Butler et al. 2012) but, based on relative proportions of the strongly asymmetrical cusps it may be based only on premolars and is therefore difficult to compare to other morganucodontans (see Discussion below).

Evidence from the abundant and often relatively complete specimens of morganucodontans recovered worldwide suggests the presence of a number of hallmark "mammalian"

characters in this non-mammalian group, such as diphyodont tooth replacement with a single generation of molars, a well-developed dentary-squamosal jaw joint, and a bulging promontorium of the petrosal encasing the cochlear duct (Rowe 1988; Wible and Hopson 1993; Rowe 1993; Rougier et al. 1996; Luo et al. 2004; Luo 2011). This character distribution outside of Crown Mammalia reinforces the importance of using well-supported phylogenetic analyses to define taxonomic groups based on membership (definition) instead of characters (diagnosis, see Rowe 1988). The dentition in morganucodontans, previously considered to require substantial remodeling through wear to achieve matching surfaces (Crompton and Jenkins 1968), did in fact have a moderate degree of occlusal precision, though less developed relative to extant mammals (Jäger et al. 2019). The molars of this group are "triconodont", with three dominant cusps arranged in a mesiodistal row. This general morphology appears in several other Mesozoic lineages (notably in "amphilestids" and eutriconodontans, which are also present in the Early Jurassic, e.g., Rougier et al. 2007a; Gaetano and Rougier 2012), but modern analyses do not support any exclusive relationship between morganucodontans and these other groups (e.g., Rougier et al. 2012). The dental pattern of *Morganucodon* (as exemplified by *Morganucodon watsoni*) is better seen as a generalized plesiomorphic pattern from which other distinctive types of molar morphologies derived, such as docodontans or "obtuse-angled symmetrodonts" (Crompton 1974; Butler 1997; Rougier et al. 2003b).

The Morrison Formation is broadly exposed across the western interior of the United States, from Montana to New Mexico. This unit is renowned for its Late Jurassic terrestrial vertebrate fauna, especially dinosaurs. Its assemblage of mammals is also relatively abundant, geographically widespread, and it is perhaps the most diverse in the world for this time period (summarized in Kielan-Jaworowska et al. 2004). The unit has been the focus of considerable exploration and study since the 1870s (e.g., Marsh 1878; Simpson 1929; Prothero 1981); the resulting mammal fauna is dominated by dryolestid and paurodontid cladotherians, docodontans, and multituberculates, with a variety of eutriconodontans and a lesser array of "symmetrodonts" also present. The majority of specimens have been recovered from sites at or near Como Bluff in southern Wyoming, consisting almost entirely of fragmentary dentaries and maxillae. Much more complete material of small vertebrates, including mammals, has been found in sites in western Colorado (Fruita Paleontological Area, Callison 1987) and northeastern Utah (Dinosaur National Monument, Engelmann and Callison 1998), but only a few of these specimens have been formally described. Notable among these, the "plagiaulacidan" multituberculate *Glirodon grandis* is known by a partial skull from Dinosaur National Monument (Engelmann and Callison 1999), a skull fragment and postcrania of the triconodontid *Priacodon fruitaensis* (Rasmussen and Callison 1981; Rougier et al. 1996; Engelmann and Callison 1998; Harper and Rougier 2019; Jäger et al. 2020), and a nearly complete,

articulated skeleton of the highly specialized and enigmatic *Fruitafossor windscheffeli* Luo and Wible, 2005, have been described from Fruita (Luo and Wible 2005).

A new small vertebrate locality, the Cisco Mammal Quarry (CMQ), was discovered in the Morrison Formation in eastern Utah in 2015, and mammals were recovered the following year (Davis et al. 2018). Preservation potential is excellent; while articulated specimens are rare, transportation and abrasion are typically minimal and three-dimensional, associated material characterizes the sample thus far. The fauna is under active study, with isolated teeth described for *Dryolestes priscus* and *Glirodon grandis* and a partial braincase possibly referrable to *Fruitafossor* sp. illustrated by Davis et al. (2018), and two isolated petrosals of uncertain affinities described by Davis et al. (2021). Here, we describe two isolated but well-preserved skull fragments of a new morganucodontan from the CMQ. Each preserves the maxilla and palatine in articulation, permitting description of portions of the snout, palate, nasal cavity, and orbital wall, as well as the entire postcanine dentition. This new taxon differs from *Morganucodon* spp. and other related taxa in the morphology of the snout and in the postcanine dentition. While the general construction of the molars is relatively conservative, there are only two molars and the posterior premolars are strongly molariform. This prompts discussion of the nature of the premolar-molar boundary in morganucodontans, and the use of wear as an indicator of the ontogenetic process of tooth replacement in identifying molars and premolars. We obtained a radiometric date for the CMQ using ashfall zircon analysis, dating the locality and its growing mammal fauna as 151.50 ± 0.28 Ma in the earliest Tithonian, Late Jurassic.

Institutional abbreviations.—NHMUK, Natural History Museum, London, UK; NLMH, Niedersächsisches Landesmuseum, Hannover, Germany; OMNH, Sam Noble Oklahoma Museum of Natural History, Norman, USA; UMZC, University Museum of Zoology, Cambridge, UK.

Other abbreviations.—CMQ, Cisco Mammal Quarry; FPA, Fruita Paleontological Area. We follow standard convention in abbreviating tooth families as I, C, P, and M, with upper and lower case letters referring to upper and lower teeth, respectively. Cranial nerves are denoted by their Roman numerals: V_2, maxillary division of trigeminal nerve; VII, facial nerve.

Nomenclatural acts.—This published work and the nomenclatural acts it contains have been registered in ZooBank: urn:lsid:zoobank.org:pub:74284503-FEC4-4BC4-9E48-768145FDC94E.

Geological setting

Rock units in the area surrounding the CMQ range from the Middle Jurassic Entrada Sandstone through the Upper

Cretaceous Mancos Shale. Exposures of the Morrison Formation in the immediate vicinity of the locality dip generally to the west at approximately 9°. The locality is at the top of an isolated, rounded knob composed of light gray silty to sandy mudstone and thin sandstone beds. The surface of the mudstone shows the "popcorn" weathering and convex slopes characteristic of mudstone that is rich in swelling clay minerals such as bentonite. Overall, the mudstone is well-cemented, calcareous, and massive, with no sedimentary structures observed. Small flecks of biotite are present, and barite nodules are common with some as large as 10 cm in diameter. The sandstone beds are more resistant to weathering than the mudstone beds and appear rounded in profile when exposed. There are distinct similarities between the lithology of the CMQ and what Kirkland (2006) described as the "drab floodplain facies" at the Fruita Paleontological Area (FPA), located approximately 48 km ENE of the CMQ. This facies displays intervals of gray mudstone with a lack of sedimentary structures interbedded with thin sandstone beds. Barite nodules occur in this facies, suggesting the occasional presence of standing water. Kirkland (2006) interpreted the strata of this facies to be deposited in smaller crevasse splays occurring seasonally on medium-sized river channels, and this interpretation is tentatively applied to the strata of the CMQ as well.

Upsection of the locality, the variegated mudstone of the Brushy Basin Member of the Morrison Formation rise to a steep cliff that is capped by the lower Yellow Cat Member of the Lower Cretaceous Cedar Mountain Formation (Kirkland et al. 2017). Downsection of the CMQ, widespread and thick sandstone channels are prominent. This lithology is typical of the Salt Wash Member (Turner and Peterson 2004) of the Morrison Formation; based on the geologic mapping of Doelling (2002), Google Earth images, and our field reconnaissance, we place the CMQ low in the Brushy Basin Member of the Morrison Formation locally. As the boundary between the Salt Wash and Brushy Basin members has been shown to be asynchronous (Trujillo and Kowallis 2015; Maidment and Muxworthy 2019), this stratigraphic placement by itself does not imply either an age nor correlation with any other localities. However, the similarities in lithology, small vertebrate fauna, and recovered age (see below) between these two geographically-proximal localities strongly suggest that CMQ and FPA were at least pericontemporaneous.

Age of the Cisco Mammal Quarry.—Mudstone samples were collected from the CMQ and were sent to the University of Wyoming Geochronology lab to evaluate for zircon crystal content and potential for dating analysis. A sample of silty mudstone taken directly from the quarry just under a productive horizon was initially processed (CMQ 190618), but this sample yielded very few zircon crystals. Most of the zircon crystals that were present were very small and rounded, suggesting a detrital origin; none had characteristics that are typical of ash-fall zircons such as longitudinal gas tracks. Two additional samples (CMQ-2 and CMQ-3) were then sent to the lab and processed, and one of these (CMQ-2) yielded enough zircons with the desired morphology to proceed (see SOM: figs. 1 and 2, Supplementary Online Material available at http://app.pan.pl/SOM/app67-Davis_etal_SOM.pdf).

Twenty-two single zircons were dissolved and analyzed by CA-ID-TIMS methods (see SOM for details on dating methodology). The weighted mean age of 151.50 ± 0.28 Ma (Tithonian, Late Jurassic) is interpreted as the best estimate of the volcanic ashfall age of the four youngest zircon crystals. The presence of rounded detrital grains and slightly older euhedral zircons, however, implies that even the youngest ages could be from detrital grains; as a result, the weighted mean represents a maximum depositional age. This age places the Cisco Mammal Quarry approximately 1 million years younger than Quarry 9 at Como Bluff (152.51 ± 0.47 Ma, Trujillo et al. 2015), and approximately 0.5 million years younger than the Main Callison Quarry at the Fruita Paleontological Area (152.0 ± 0.3 Ma, Foster et al. 2017). However, it should be noted that the ranges of these ages do overlap leaving open the possibility that CMQ and FPA are contemporaneous.

Material and methods

The two skull fragments described here were recovered from the Cisco Mammal Quarry in 2016 via hand quarrying. Each specimen was split during discovery into part and counterpart, which were reunited using Butvar and mechanically prepared with a carbide needle under magnification. One specimen was figured but not described in the initial report of the locality (Davis et al. 2018: fig. 4C). OMNH 80538 (holotype) was scanned at the University of Texas High-Resolution X-Ray CT Facility using a Zeiss Xradia with a voxel size of 11.3 μm; OMNH 69352 was scanned at the Institute of Geosciences, University of Bonn, using a v|tome|x s μCT device (GE Sensing & Inspection Technologies GmbH phoenix|x-ray) with a voxel size of 30.5 μm. 3D data visualization and digital segmentation were performed in Avizo (Thermo Fisher Scientific) and Polyworks (InnovMetric Software Inc.). For the descriptions of tooth crown morphology, we prefer to employ dental terminology that is based on an hypothesis of homology across mammaliaform groups, where possible. Serial homology of the primary upper premolar cusp, the large central cusp of "triconodont" and "symmetrodont" molars (traditionally labeled cusp A), and the paracone of therian molars is well established (e.g., Butler 1939; Patterson 1956), but differing interpretations exist regarding the large flanking upper molar cusps and accessory cusps in taxa with "triconodont" dentitions, labeled B–E in traditional nomenclature (Crompton and Jenkins 1968). We choose to follow Rougier et al. (2003b, see references therein) in identification of cusps on upper teeth.
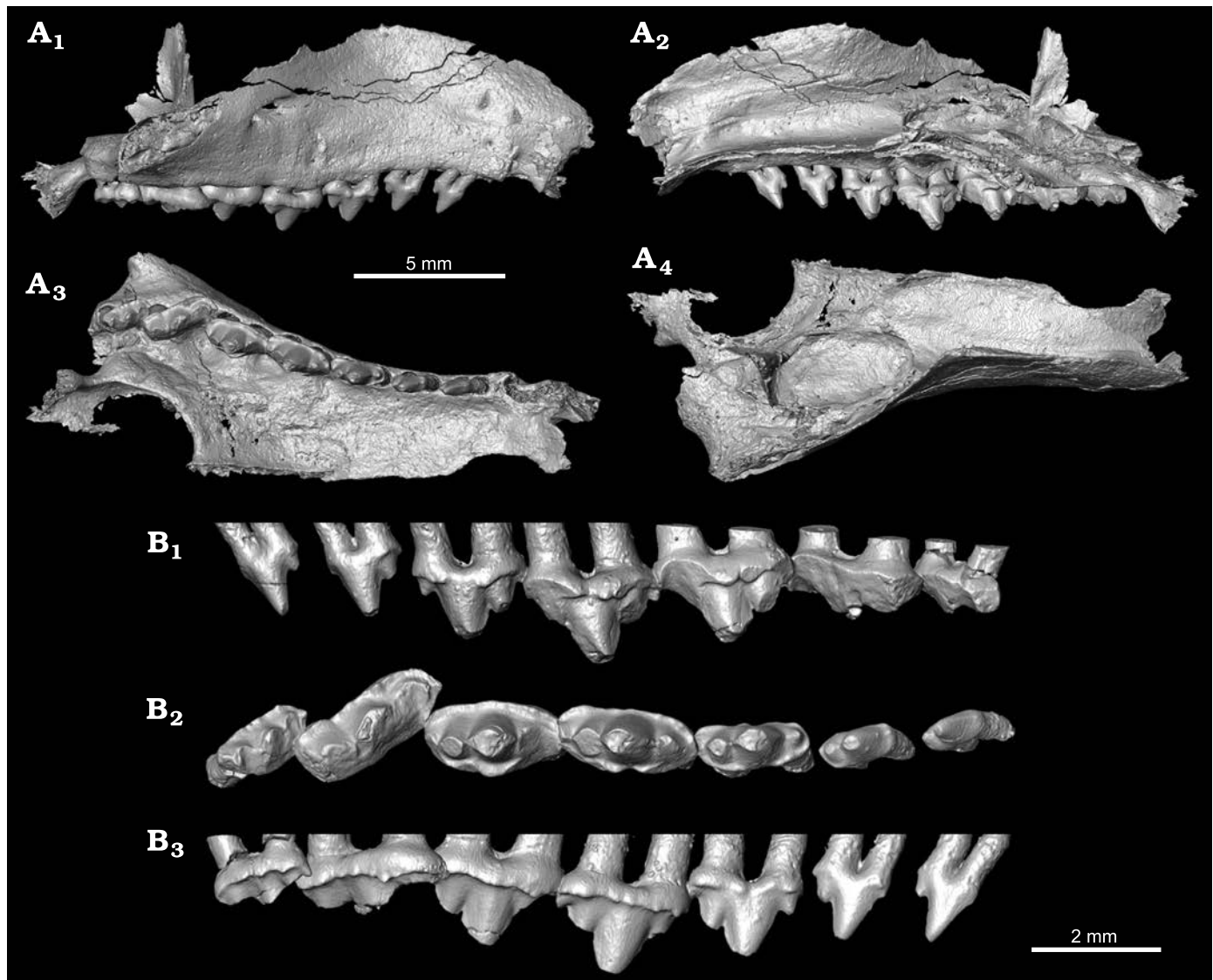
Fig. 1. 3D surface renderings from CT data of the morganucodontan mammaliaform *Cifellilestes ciscoensis* gen. et sp. nov. (OMNH 80538, holotype), from the Cisco Mammal Quarry, Utah, USA, Upper Jurassic Morrison Formation. **A**. Right skull fragment in lateral (A_1), medial (A_2), ventral (A_3), and dorsal (A_4) views. **B**. Dentition only in lingual (B_1), occlusal (B_2), and buccal (B_3) views.

Systematic palaeontology

Mammaliaformes Rowe, 1988

Morganucodonta Kermack, Mussett, and Rigney, 1973

Genus *Cifellilestes* nov.

Type species: *Cifellilestes ciscoensis* sp. nov., monotypic, see below.

Zoobank LSID: urn:lsid:zoobank.org:act:90CAB130-51C1-4CE7-BBE1-6D8CD36CEEFD

Etymology: In honor of Richard Cifelli for his contributions to our understanding of Mesozoic mammals, especially through decades of field efforts to improve the fossil record; and Greek *lestes*, thief, a common suffix for fossil mammals.

Cifellilestes ciscoensis sp. nov.

Zoobank LSID: urn:lsid:zoobank.org:act:801C5454-4299-4352-AB6E-E78CC923810D

Etymology: In reference to the ghost town of Cisco, Utah, close to the type locality to which it also lends its name.

Holotype: OMNH 80538, right skull fragment preserving partial palate and snout, and postcanine dentition.

Type locality: OMNH V1728, Cisco Mammal Quarry, Grand County, Utah, USA.

Type horizon: Brushy Basin Member of Morrison Formation, Tithonian, Upper Jurassic.

Material.—Holotype and OMNH 69352, left skull fragment preserving partial palate and snout, and postcanine dentition; from type locality and horizon.

Diagnosis.—Upper molariforms with three primary cusps arranged in a line, but differing from eutriconodontans and resembling morganucodontans in the presence of complete, cuspidate lingual and buccal cingula and the absence of interlock between adjacent molars; resembles species of
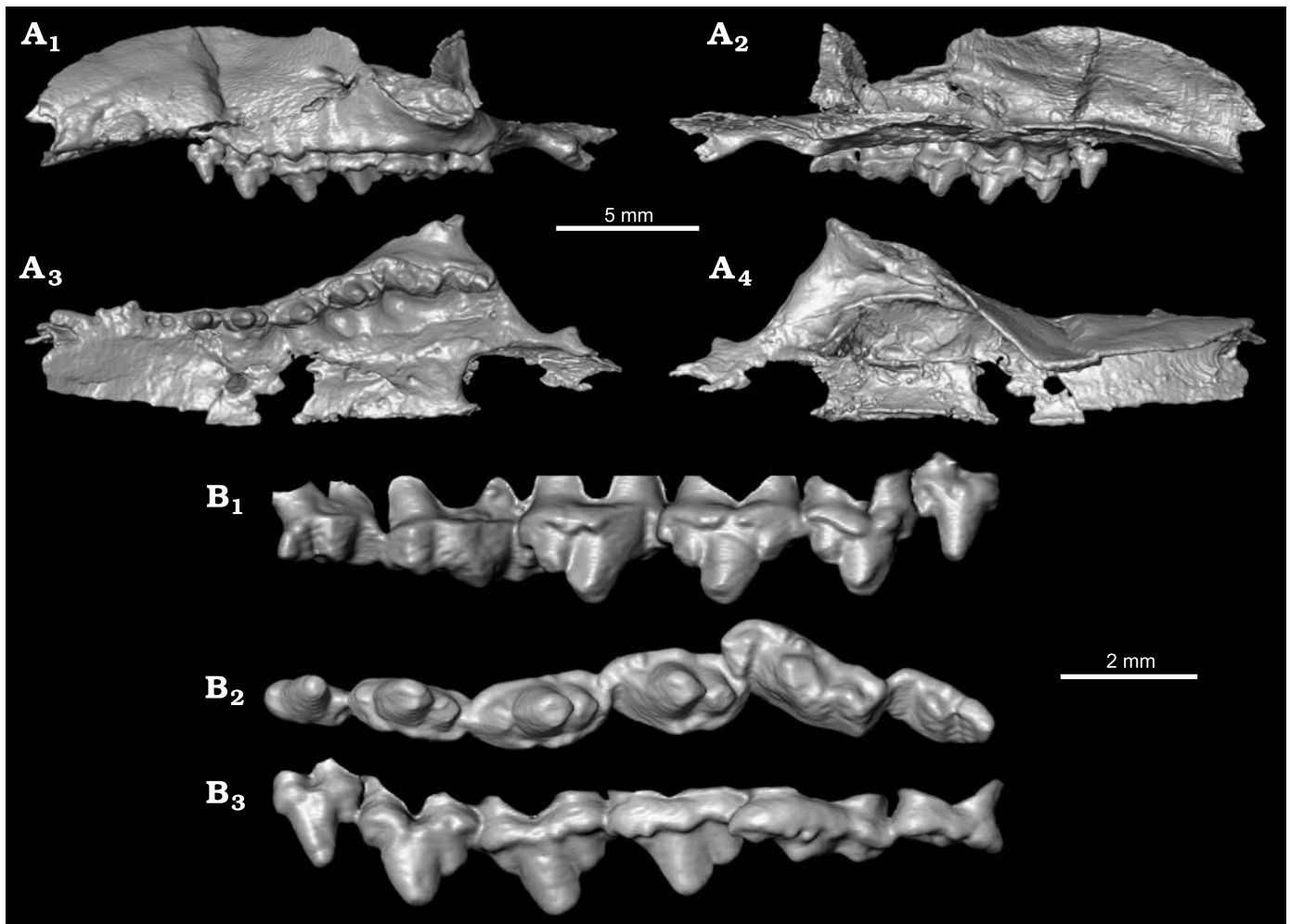
Fig. 2. 3D surface renderings from CT data of the morganucodontan mammaliaform *Cifellilestes ciscoensis* gen. et sp. nov. (OMNH 69352), from the Cisco Mammal Quarry, Utah, USA, Upper Jurassic Morrison Formation. **A**. Left skull fragment in lateral (A$_1$), medial (A$_2$), ventral (A$_3$), and dorsal (A$_4$) views. **B**. Dentition only in lingual (B$_1$), occlusal (B$_2$), and buccal (B$_3$) views.

Morganucodon but differs from other morganucodontans in pronounced imbrication of distal upper teeth; differs from known morganucodontans in presence of only two molars, molarization of distal three premolars, presence of a single, large infraorbital foramen, and of a buccinator ridge on the lateral alveolar margin of the maxilla.

Description.—Both specimens, left and right skull fragments, preserve a nearly complete maxilla and much of the palatine. Both specimens are broken in a strikingly similar manner with only minor differences in morphology (Figs. 1, 2); however, minor differences in size and degree of tooth wear preclude referral to the same individual. Both specimens are presumed to be adults based on the heavy wear of the ultimate molar and the absence of replacement teeth within the maxilla. OMNH 69352 is slightly larger than the holotype based on the length of the postcanine alveoli and shows a slightly more advanced stage of tooth wear (though some details of the pattern are not identical), suggesting this specimen represents an older individual. The dentition is better preserved in the holotype (OMNH 80538), and that specimen will be the focus of the descrip-

tion with differences in morphology between the two specimens noted where they occur. The well-preserved facets for the jugal and lacrimal as well as the three-dimensional preservation of the delicate orbital and pterygoid processes of the palatine (though damaged) suggest that these specimens were gently disarticulated from their adjacent skull elements during deposition (Fig. 3). Some low-energy transport occurred as the specimens were isolated. While the referred specimen was identified as a mammal maxilla in the field, the holotype was only recognized after some mechanical preparation following the field season; we therefore have no record of how close to one another the specimens were recovered.

Lateral view: The maxilla appears to be nearly complete except for some breakage anteriorly in the vicinity of the canine alveolus and some likely minor breakage along the area interpreted as the suture with the nasal (Fig. 4). The facial process of the maxilla is nearly vertical and convex dorsally, tapering in lateral view posteriorly to a low, laterally flaring base for the zygomatic arch and anteriorly to the presumed contact with the premaxilla (though the suture is not pre-
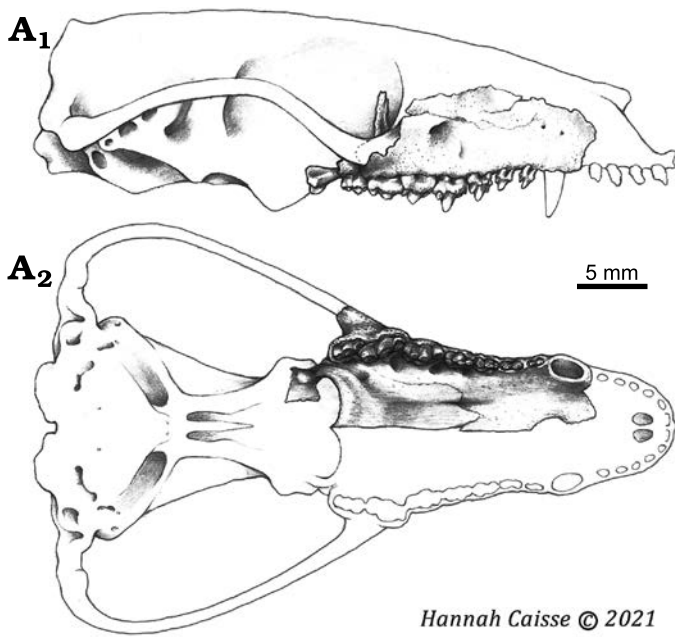
Fig. 3. Hypothesized life position of the skull fragment (OMNH 80538) of the morganucodontan mammaliaform *Cifellilestes ciscoensis* gen. et sp. nov., in lateral (A_1) and ventral (A_2) views. Remainder of the skull based on the composite restoration of *Morganucodon* by Kermack et al. (1981). Artwork by Hannah Caisse.

served in either specimen). The maxilla includes the entirety of the single large canine alveolus, and no incisor alveoli are preserved within the maxilla in contrast with the condition in *Morganucodon watsoni* Kühne, 1949, and docodontans (Kermack et al. 1973; Lillegraven and Krusat 1991; Rougier et al. 2014). The dorsal portion of the facial process curves slightly medially, resulting in a tall rostrum only slightly rounded towards the presumed contact with the nasals. Most of the curved dorsal edge of the maxilla is interpreted as the natural margin of the suture with the nasal, and the shape of this margin suggests the nasals were wider posteriorly than anteriorly. The prong along the dorsal margin directly above the P4 is here interpreted as the position where contact occurred with the nasal anteriorly and the lacrimal posteriorly (Figs. $1A_1$, $4A_1$). Low on the maxilla and stretching about the length of the two molars there is a well textured, oval facet in the maxilla that continues posteriorly following the overhang of the zygomatic process and the maxillary tuberosity. Most of the large, dorsolaterally-facing facet was likely occupied by the jugal, leaving only a small contact area for the lacrimal immediately dorsal to the infraorbital foramen. The maxilla continues posteriorly beyond the base of the zygoma, with the distal root of the ultimate molar fully posterior to the contact with the jugal. There is little bone posterior to this in either specimen, suggesting these are adults and no additional teeth would be expected. There is a single large, anteroposteriorly elongate infraorbital foramen, positioned dorsal to the mesial root of the P5 or between the P4 and P5 (Figs. $1A_1$, $2A_1$, $4A_1$). However, the medial and lateral walls of the foramen bear low ridges that give it a faint figure-eight shape in coronal section. The direction of the infraorbital

canal and foramen suggest that the infraorbital branch of V_2 and accompanying vessels were directed anteriorly, high on the rostrum in the direction of the postcanine recess. Though the lateral wall of the canine alveolus is crushed, there is no indication of a large boss for the canine root, suggesting that this tooth was moderate in size. There are three small foramina on the lateral snout, one dorsal to the canine, one dorsal to the mesial root of the P1, and a third smaller one in between and ventral to these. These open into the alveolar canal and would likely have transmitted blood vessels and/or small branches of V_2, as in non-mammaliaform cynodonts (see discussion of the rostral alveolar canal and foramen in Benoit et al. 2016b, 2020). As these foramina are well removed anteriorly from the primary opening of the infraorbital canal, we do not consider them to represent additional infraorbital foramina. A distinct, thickened ridge contours dorsally along the rim of the alveolar process; this is the buccinator ridge, which is particularly distinct between the P1–M1. The size and orientation of the infraorbital foramen and the clear buccinator ridge indicate the presence of fleshy cheeks in *Cifellilestes* gen. nov. (as seen in extant mammals, e.g., Pietrokovski and Massler 1967).

Ventral view: The bony palate preserves contributions from the maxilla and palatine (Fig. $4A_3$). The palatal process of the maxilla is broken and displaced in some parts, but some portions of the midline suture are preserved. No portion of the incisive foramen is preserved. Though crushed laterally, the single canine alveolus appears to be complete or nearly complete and we interpret it was entirely housed within the maxilla. The zygomatic process of the maxilla is well exposed in ventral view with its lateral-most extent even with the mesial root of the M2; most of the crown of this tooth is posterior to the anterior root of the zygomatic arch. The maxillary tuberosity is present on the narrow rim of bone posterior to the M2. There are substantial pits present just medial to the roots of the posterior dentition to accommodate the protoconids of the lower teeth, which must have been conical and quite tall. The first and shallowest of these pits is positioned between the P3–P4, with the posteriormost between the molars also rather shallow. The pits between the P4–P5 and P5–M1 are very deep, with the latter the deepest. The maxilla–palatine suture is nearly transverse at its most medial point, even with the paracone of the P3. From there, the suture arcs posterolaterally just medial to the palatal pits. The palatine has been displaced by breakage in the holotype but is preserved in-situ in the referred specimen. The posterior margin of the bony palate curves medially to a prominent posterior nasal spine, positioned even with the M1–M2 boundary. It appears that the posterior end of the bony palate in the holotype may have been positioned slightly more anteriorly, perhaps a half-tooth length, though this is uncertain due to some displacement of the palatine due to breakage (Figs. $1A_3$, $2A_3$). The referred specimen is undistorted here, and the posterior margin of the bony palate reaches the anterior half of the ultimate molar (Fig. $2A_3$). The greater palatine foramen is positioned on the maxilla–
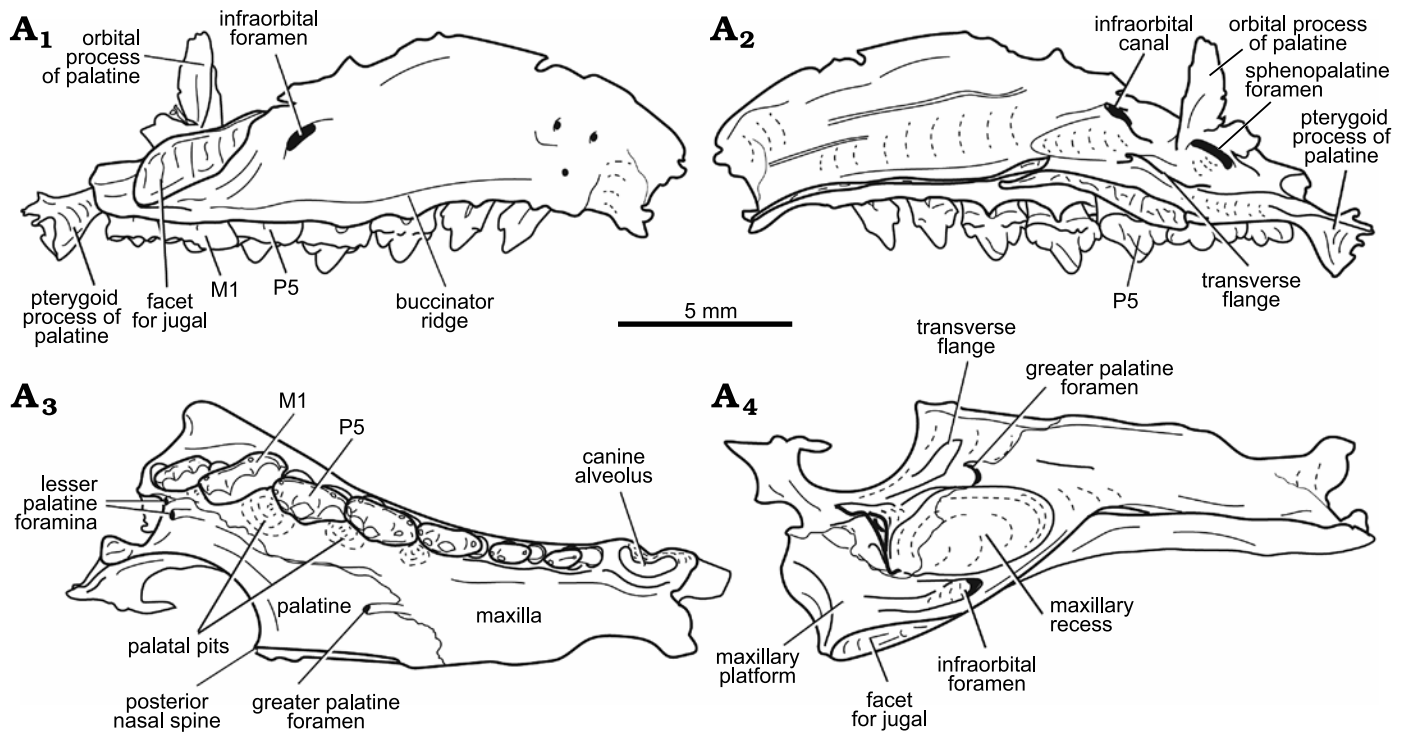
Fig. 4. Illustration of the morganucodontan mammaliaform *Cifellilestes ciscoensis* gen. et sp. nov. (OMNH 80538, holotype); right skull fragment in lateral (A_1), medial (A_2), ventral (A_3), and dorsal (A_4) views.

palatine suture, at the level of the P4. A prominent groove continues anteriorly from this opening. Two lesser palatine foramina are present on the holotype, directed anteriorly on a horizontal plane and opening just medial to the distal root of the ultimate molar (only one lesser palatine foramen is present on the referred specimen). Only a thin bridge of bone encloses these foramina ventrally, and prominent grooves extend from them anteriorly on the palate. Posteriorly from the lateral margin of the palate, the palatine tapers before flaring into a club-shaped pterygoid process. The narrowed neck of this region of the palatine is laterally convex and medially concave, where it frames the margin of the choana. A thin, sub-horizontal plate of bone is present dorsally where the palatine would have met the sphenoid complex in the mesocranium. Posteriorly, the presumed contact with the pterygoid is complex; a thin vertical ridge extends posteriorly on the medial side, while a blunt, triangular knob is present more anteriorly and projects laterally. This knob supports a low crest and delimits a shallow pocket on the posterolateral surface of the pterygoid process, and we interpret this to be a complex articulation with what would have likely been a heavy pterygoid element or perhaps even the alisphenoid. While unclear due to preservation, the pterygoid ramus of the alisphenoid would likely have overlapped at least to some extent this club-shaped structure dorsally. This arrangement of the sidewall of the choanae is similar to that described for some close non-mammaliaform outgroups, such as *Chaliminia musteloides* Bonaparte, 1980, and species of *Massetognathus*, among others (Martinelli

and Rougier 2007; Rowe and Shepherd 2016; Crompton et al. 2017).

Orbit: Very little of the orbit is preserved, only the contribution by the maxilla and part (presumably) of the orbital process of the palatine. The maxilla forms a horizontal shelf in the anterior floor of the orbit (the orbital platform), medial to the root of the zygoma. The roots of the molars do not pierce the maxillary platform and cannot be seen in the orbit. The posterior opening of the infraorbital canal, the maxillary foramen, is present on the orbital platform (Fig. 4A_4); the dorsal rim of the canal was likely formed by the lacrimal but is not preserved. This canal is preserved in both specimens as a well-defined but dorsally open trough within the maxilla between the floor of the orbit and the opening onto the face, and is only briefly enclosed by the maxilla as it exits anteriorly. There are one or two small foramina on the maxillary platform posterior to the maxillary foramen that travel anteroventrally to communicate with the alveolar canal; these likely held small (perhaps middle alveolar) branches of V_2. The infraorbital canal communicates with the remaining anterior portion of the alveolar canal through a small passageway just prior to its exit onto the face (visible in CT slices). The preserved portion of the orbital process of the palatine is tall, extending vertically above the level of the presumed contact between the maxilla and nasal (Fig. 4A_1). It forms a right angle in horizontal section, with a thin lateral process oriented towards the position of the lacrimal and a thin plate that would have formed a portion of the medial orbital wall. Breakage precludes any estimate of contact with other bones expected in this region, such as

the frontal or orbitosphenoid, but the height of the orbital process suggests that the palatine formed a considerable portion of the medial wall of the orbit. The nasal cavity and the orbit were separated by a full bony wall that, in addition to the maxilla, a large palatine, and the lacrimal, likely also included the now missing frontal. Transmission of neurovascular structures between the two regions would have been accomplished via distinct, relatively small foramina as in modern mammals. A large, oval-shaped sphenopalatine foramen is preserved, opening into the nasal cavity medial to the base of the orbital process of the palatine (Fig. 4A$_2$). The floor of this foramen in the referred specimen is divided into a pair of grooves. This foramen would have transmitted neurovasculature from V$_2$ (plus autonomic fibers from the greater petrosal branch of VII) and the maxillary artery to the nasal cavity and palate, as occurs in living mammals.

Nasal cavity: The nasal cavity is tall and broad posteriorly, and while seeming to retain much of its height anteriorly (though the frontals and nasals are not preserved), a narrowing of the snout anterior to the infraorbital foramen sharply reduces the width of the nasal cavity. A prominent oval pocket occupies the posterolateral floor of the nasal cavity, immediately anterior to the orbital process of the palatine. This is identified as the maxillary recess (following Crompton et al. 2017). The maxilla–palatine suture is interpreted to pass obliquely across the posterior third of the maxillary recess. No turbinals are preserved. Three parallel grooves are visible coursing along the lateral wall of the nasal cavity (Fig. 4A$_2$). The superior two of these likely represent attachment sites for maxilloturbinals, and the inferiormost groove was likely for the nasolacrimal duct. A thin but prominent transverse flange is preserved extending medially from near the base of the orbital process of the palatine (Fig. 4A$_2$) (see terminology in Maier 1993). It passes parallel to the palatal process of the palatine; this shelf would likely have contacted the vomer, as in species of *Morganucodon* and close sister taxa (Kermack et al. 1981; Crompton et al. 2017). Here, the transverse flange would delimit a rather shallow inferior air passage at the rear of the nasal cavity (which communicated through the choana into the pharynx) and also formed the floor of the sphenoidal recess at the posterodorsal extent of the nasal cavity. The sphenopalatine foramen opens anteromedially into the nasal cavity adjacent to the base of the transverse flange. A groove connects the foramen with the dorsal opening of the greater palatine foramen, which is positioned along the maxilla–palatine suture and directed anteriorly (Fig. 4A$_4$). The infraorbital canal is interpreted to have lacked exposure to the nasal cavity. There is no evidence of a maxillary sinus developed in the substance of the maxilla.

Dentition: Upper dental formula is interpreted as ?.1.5.2 (see Table 1 for tooth measurements). No incisor alveoli are preserved in the maxilla though it is uncertain if the maxilla continued anteriorly from the preserved margin around the canine alveolus. The canine is represented by a single, large, elliptical alveolus (Figs. 1A$_3$, 4A$_3$); though crushed

Table 1. Measurements (in mm) of crown lengths (mesiodistal) and transverse widths (through the widest point of the paracone base) of the morganucodontan mammaliaform *Cifellilestes ciscoensis* gen. et sp. nov., from the Upper Jurassic Morrison Formation of Utah, USA. Brackets indicate truncation due to wear.

	OMNH 80538 (holotype)		OMNH 69352	
	length	width	length	width
P1	1.07	0.49	–	–
P2	1.24	0.55	1.33	0.59
P3	1.87	0.69	1.81	0.76
P4	2.25	0.96	2.20	0.92
P5	2.26	1.22	2.23	1.19
M1	[2.59]	[1.06]	[2.60]	[1.03]
M2	1.68	[0.86]	1.72	[0.83]

on both specimens, there is no indication that this alveolus was divided and root length and proportions compared with *Morganucodon* spp. suggest the tooth was single rooted. Five double-rooted premolars are present, all of which have a short crest bridging the roots at the base of the crown. None of the postcanine teeth show evidence of apical expansion of the roots, nor are the roots fused for any portion of their length. The referred specimen bears a distinct diastema between the canine and P1 (Fig. 2A$_3$), and the alveolar bone in this region is textured and appears modified as would be expected if a tooth position had been shed without replacement. CT data appear similar but do not reveal evidence of alveoli or roots in this region, and the holotype lacks a diastema. We therefore interpret this as a variable presence of a C–P1 diastema, perhaps related to the age (based on tooth wear) and larger size of the referred specimen, instead of evidence of loss of a mesial premolar position. The premolars gradually increase in size and complexity distally (Fig. 1B).

Figure 5 illustrates our cusp nomenclature for the postcanine teeth, as outlined above in the Materials and conventions section. The P1 is small, simple, and premolariform, with a somewhat laterally compressed paracone and a much lower but still well-developed distal heel cusp; we identify this as the metacone. A faint bulge is present at the distalmost edge of the crown; this bulge transitions to a substantial cingular
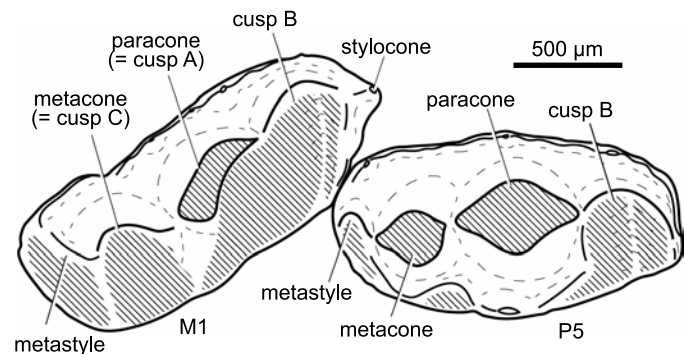

Fig. 5. Illustration of crown morphology of the morganucodontan mammaliaform *Cifellilestes ciscoensis* gen. et sp. nov. (OMNH 80538 (holotype); right P5–M1 in occlusal view. Terms in parentheses label homologs with traditional "triconodont" cusp nomenclature (e.g., Crompton and Jenkins 1968; Rougier et al. 2007a).

cusp through the premolar series and is here interpreted as the metastyle. A very faint bump is present on the mesial crown base; on distal teeth, we identify the cusp in this position as cusp B. The P2 is also premolariform but its cusps are more robust, with the metacone much larger than on the P1. The metastyle is still low but it is connected to a cingulum that rings the lingual base of the metacone before fading. The B cusp is slightly better defined than on the P1 but still minute, and while a faint cuspule is visible at the mesiobuccal corner of the crown no buccal cingulum is present. The distal root is slightly larger than the mesial root on the P1 and P2. The morphology of the P3 is substantially different from the mesial premolars. The paracone is taller and heavier, with a strong distal crest meeting a large but still much lower metacone. The bases of these two cusps are poorly separated. Cusp B is by far the lowest of the three main cusps and is somewhat mesially inclined, though this cusp is proportionately larger than in the P2 and its base more elevated and detached from the cingulum. The P3 metastyle is much larger than on the P2 but it is wedged against the base of the P4. This relationship is present in both specimens, suggesting that this represents the fully erupted position of the tooth (Figs. 1B, 2B). A distinct cingulum is developed mesially and distally on the P3, but it is incomplete at the mid-point of the crown both buccally and lingually at the base of the paracone. Small cuspules are present along the cingula. The paracone and metacone have apical damage but also show evidence of wear; there is a narrow facet developed on the mesiolingual face of the paracone, and the metacone is beveled in an orientation that suggests contact with the paraconid of the lower p4 (a small patch of wear is also present along the distal lingual cingulum on the P3 of the holotype, though this facet is absent from the referred specimen; see discussion of wear and occlusion below). The P4 continues the trend of increasing size and molarization of the premolars. The tooth and its major cusps are arranged along the main axis of the tooth row. The B cusp and metacone are larger than on the P3, but the apices of the three main cusps are close to each other and their bases remain poorly separated. The large, round paracone base occupies most of the crown width. The metastyle is large and connected to the metacone by a sharp crest; the distal face of this cusp has been removed by wear. The mesial-most portion of the crown is too worn to determine if an additional cusp was present (this cusp would be homologous with the stylocone) but, judging from the size of this cusp on the molars where it is preserved, it would likely have been tiny. A complete buccal cingulum is present and bears several small cuspules, the largest of which are at the mesial and distal ends where the cingulum is the broadest. The lingual cingulum is nearly complete except for a small gap lingual to the apex of the paracone (we assume the presence of this cingulum mesially, as it is present on the P3); two or three heavy cuspules were likely present adjacent to the base of the paracone, but portions are heavily worn. While apical wear of the P4 paracone is similar to that on the P3, there is considerably more occlusal wear on the me-

siolingual and distolingual flanks of the P4 crown. A large facet is present on the mesial slope of the paracone lingual to the main crest, and a roughly coplanar facet occupies the mesiolingual corner of the crown base. The B cusp has been abraded obliquely, and the cingulum has been obliterated here. Distally, much of the metacone has been removed by wear leaving an oblique, lingually-oriented surface and significant wear is present along the distolingual cingulum (though the cingulum is still distinct). The P5 is very similar to the P4 in overall proportions, differing in aspects of the cingula and in wear pattern (see discussion below). The buccal cingulum is comparatively wider at the level of the paracone base than on the P4, and the lingual cingulum is complete. A large lingual cingular cusp is present centrally, even with the apex of the paracone. The cingulum mesial to this has been obliterated by wear, and a second large, worn cingular cusp is present distally. Cusp B has been almost completely removed by a deeply incised groove cut into the crown by the p5 protoconid, and much of the metastyle and part of the distal lingual cingulum have been flattened by a distolingually-oriented wear facet (Figs. 1B, 5).

The molars are sharply imbricated relative to the premolars, with the line of their cusps rotated distolingually (Figs. 1B, 2B, 5). Both molars also bear a very low crest bridging the roots. While heavily worn, the relative proportions of the three main cusps on the molars appear to have been different from the premolars—the paracone was still likely the tallest cusp, but the bases of the three cusps are much better separated and have a similar buccal extent, giving the crown a roughly rectangular footprint rather than the elliptical shape of the distal premolars. It also seems likely that the paracone of the P4 and P5 was taller than that of the molars, though wear and breakage leave some uncertainty. As preserved, the M1 is the mesiodistally longest tooth of the series (it is unclear how much of the distal crown has been removed by wear). Judging by their bases cusp B was subequal to the metacone, but substantial wear makes cusp heights impossible to determine with certainty. Cusp B is heavily excavated by wear, similar to P5 (Fig. 5). A small but distinct stylocone is present at the mesial end of the crown, in line with the main cusps and connected to the base of cusp B by a faint crest. The stylocone anchors what remains of the lingual cingulum, which is present only at the mesiolingual corner where the M1 and P5 are in contact. The remainder of the lingual cingulum, along with at least the lingual halves of the paracone and metacone, have been obliterated by wear. The buccal cingulum is complete, well developed, and cuspidate along most of its length. A large cuspule is present at a level between the bases of cusp B and the paracone. The distal end of the crown has been flattened by wear in a plane perpendicular to the line of the main cusps; this margin appears to stop at a crest connected to the metacone and coursing to the distobuccal corner of the crown. The orientation of this crest suggests that the metastyle may have been positioned at this corner instead of in-line with the main cusps, as it is on the premolars. A similar

morphology of this crest is present on the M2, supporting deviation of the position of the metastyle. The M2 is a much smaller tooth, about 60% the length of the M1. It is more compact in overall shape, but this is perhaps due to differences in relative wear pattern; both molars show a similar amount of wear indicating that the specimen is a senescent individual. Cusp B is proportionally smaller on M2 than on M1, the buccal cingulum lacks a dominant cuspule, and is slightly narrower distally, but the molars are otherwise generally similar. There is some evidence of wear on the distal face of the M2 in the holotype specimen suggesting the presence of an additional lower molar (an m3), but this could instead represent damage (a facet does not appear to be present on OMNH 69352).

Stratigraphic and geographic range.—Type locality and horizon only.

Discussion

Interpretation of dental formula.—The establishment of diphyodonty, which differentiates the postcanine dentition into molars and premolars, is a hallmark character that has historically been associated with Mammalia (e.g., Rowe 1988: table 1). Molars, by definition, are teeth derived from the primary dentition that are not replaced—any tooth posterior to the last replaced tooth is a molar (based on Owen 1868; see also Bi et al. 2016). As this definition relies on an ontogenetic process (tooth replacement) that is rarely preserved directly, indirect evidence is often employed in identification of the premolar/molar boundary in most taxa. In the absence of teeth preserved in the process of eruption, the most reliable indicator of replacement timing or sequence is wear (Rougier et al. 2003a; Rougier et al. 2007b; Davis 2011; Lopatin and Averianov 2015; Martinelli et al. 2021). The relative accumulation of wear can be used to identify teeth that have been replaced or the sequence in which teeth have erupted (see Luckett 1993). Additional support can come from crown morphology; traditionally, a major transition in form within the postcanine dentition has been used to establish the premolar/molar boundary (e.g., "triconodonts", Osborn 1888; Trinity therians, Slaughter 1981), with molars typically being markedly more complex than permanent premolars. This approach has several potential sources of problems and inconsistencies; it is problematic in taxa with molariform premolars (e.g., Lopatin et al. 2010; Davis 2011; Bi et al. 2016) and in groups with hypothesized loss of replacement of molariform deciduous premolars (e.g., Metatheria, McKenna 1975). The phylogenetic signal of this feature is another potential source of conflict. Many non-mammaliaform cynodonts achieve a distally increasing gradient of morphological complexity in the postcanine dentition (Martinelli et al. 2017; O'Meara et al. 2018) but replacement of all loci appears to be retained. At some point in the mammaliaform lineage diphyodonty was established, but given that all postcanines developed from a single precursor from the dental lamina there is no reason a priori to assume that diphyodonty was established at once on several loci of the posterior dentition. It is conceivable that molar differentiation begins distally by suppressing eruption of the replacement dentition and phylogenetically progresses mesially affecting other loci. Gobiconodontids show replacement of teeth that morphologically had traditionally been considered as molars (Jenkins and Schaff 1988; Lopatin and Averianov 2015), but are more appropriately considered as premolars based on the above definition. A low number of molars may result from specialization but depending on the phylogenetic context it may reflect an expected plesiomorphic or apomorphic condition.

Both specimens of *Cifellilestes ciscoensis* gen. et sp. nov. are adults with no evidence of developing tooth germs for additional molars or replacement premolars. Crown morphology provides some equivocal data, so our identification of the premolar/molar boundary must rely on evidence from relative wear. The anterior two postcanine teeth are small, simple in lacking buccal and lingual cingula, and are premolariform in their cusp proportions (Figs. 1B, 2B); these are clearly premolars. The posteriormost two teeth are imbricated, have additional accessory cusps and complete, cuspidate cingula, and are molariform in that the three main cusps are well-separated and roughly similar in size; these are congruent with teeth identified as molars in other morganucodontans (Crompton 1974; Parrington 1978; Jenkins et al. 1983; Gow 1986; Crompton and Luo 1993). The central three postcanine teeth form a smooth morphological gradient of increasing size and complexity, being much more complex than the anterior premolars but somewhat less complex than the molars. Distinct breaks in morphology occur distal to the P2 (start of molarization) and again at the penultimate tooth where crown morphology changes and the occlusal relationship with the lower dentition shifts substantially (as indicated by imbrication of the last two teeth). Tooth wear shows a similar pattern; the last two teeth are substantially more worn than any others, with much of their main cusps leveled and the entire lingual cingulum obliterated. The anterior three teeth show primarily apical, non-occlusal wear and lack evidence of complex occlusion with the lower dentition, as would be expected for premolars. The fourth and fifth postcanine teeth bear large facets for embrasure wear from large lower antagonists and while a deep groove has been cut into cusp B of the antepenultimate tooth, these two teeth are substantially less worn than the definitive molars behind them. Both retain much of the lingual cingulum and the lingual bases of the paracone and metacone are still intact.

We interpret the postcanine formula in *Cifellilestes* gen. nov. as P5–M2 which, although unusual, is in congruence with both relative wear and crown morphological data (Fig. 6). The sharpest change in morphology occurs at what we regard as the premolar/molar boundary: the P5/M1 transition. The M1 is the longest tooth (Table 1) but is lower crowned and has quite different cusp proportions than the P5, with the bases of cusp B and the metacone

Fig. 6. Comparative 3D renderings of upper dentition of the morganucodontans *Morganucodon watsoni* Kühne, 1949 (**A**, UMZC Eo.CR.1, reversed; Lower Jurassic fissure fills, Wales, UK), *Storchodon cingulatus* Martin, Averianov, Jäger, Schwermann, and Wings, 2019 (**B**, NLMH 105654; Upper Jurassic Süntel Formation, Germany), *Megazostrodon rudnerae* Crompton and Jenkins, 1968 (**C**, NHMUK PV M 26407; Lower Jurassic Stormberg Group, Lesotho), and *Cifellilestes ciscoensis* gen. et sp. nov. (**D**, OMNH 80538, holotype; Upper Jurassic Morrison Formation, USA), in lingual (A_1–D_1) and occlusal (A_2–D_2) views. White lines indicate the premolar–molar boundary (all taxa except *Storchodon*, which is known by only a single molar). This boundary is marked by a tall-crowned ultimate premolar with much lower flanking cusps followed by a first molar that is comparatively lower crowned with less height difference between the main cusps. Note imbrication of the molars in *C. ciscoensis* gen. et sp. nov. (D_2) and distal molars in *Mo. watsoni* (A_2), a feature absent in *Me. rudnerae* (C_2).

much better separated from the paracone (the three main cusps of the distal premolars are more closely approximated by comparison with the molars). The premolars are all roughly in-line mesiodistally with one another while the molars are strongly imbricated, suggesting a major shift in occlusal relationships between P5 and M1. A gradual increase in size and molarization is present through the entire premolar series, with the largest change occurring between P2 and P3 but this primarily concerns development of the cingula and increase in size of the flanking cusps; we consider the P3 as a weakly molarized premolar in that the metacone is robust but the B cusp is still quite

small, and both buccal and lingual cingula are interrupted at their midpoints. The P4 and P5 are more strongly molariform but differ from the P3 only in regard to overall size and in completeness of the cingula (the height of cusp B cannot be evaluated due to heavy wear). The two molars are the most heavily worn teeth in both specimens, and the contrast with the preceding tooth is so stark that concluding that the anterior teeth have been replaced seems to be the only option to explain it. Therefore, a break occurred in the developmental control of the five mesial teeth with regards to the ultimate two. The lower m1 protoconid was likely massive judging by the size of the palatal pit be-

tween P5 and M1, and occlusion with the distal face of this lower molar has removed most of the mesiolingual portion of the M1. The adjacent facet for the mesial face of the m1 protoconid on the P5 is comparatively far less developed and is restricted to the metastyle and part of the cingulum. Placement of the premolar/molar boundary between the fifth and sixth postcanines, resulting in a count of P5–M2, is best supported by available data from relative tooth wear and also from morphology.

Alternative interpretations are possible but we consider them unlikely. The P4 and P5 could be molars, yielding a formula of P3–M4. Both of these teeth have a complete buccal cingulum; the presence of a complete buccal cingulum was used as a supporting feature to distinguish the M1 from the P4 in *Morganucodon oehleri* Rigney, 1963, by Luo et al. (1995), but the P3 in *Cifellilestes ciscoensis* gen. et sp. nov. has a nearly complete cingulum, as well. The P4 and P5 are noticeably more worn than the anterior premolars which, under an alternative interpretation that these are molars, supports a lack of replacement at these two positions. As noted above, the P4 and P5 are less worn than the M1 and M2, supporting their identification as premolars. It should be noted that the distribution of wear on molars in early mammaliaforms is variable and does not always strictly follow the eruption sequence. Jäger et al. (2019) showed that M1 in some specimens of *Morganucodon watsoni* can be less worn than the posterior molars, due to a shift in occlusal relationships following the eruption of larger posterior molars. A similar pattern has been described for *Haldanodon exspectatus* Kühne and Krusat, 1972, where the posterior molars of some specimen show considerably more wear than the anterior ones (Brinkkötter 2019). The wear pattern of P4 and P5 in *Cifellilestes ciscoensis* gen. et sp. nov. is generally similar to that of molars in species of *Morganucodon* (see section on facet analysis below) and the deep maxillary pits tend to be associated with molar positions in most taxa (though they can be found at every postcanine position, e.g., the zhangheotheriid *Anebodon luoi* Bi, Zheng, Meng, Wang, Robinson, and Davis, 2016). While there is some evidence based on details of wear pattern to consider P4 and P5 as instead molars, the morphological evidence is limited to the presence of complete buccal and lingual cingula on these teeth. The progressive molarization through the postcanine series and the morphological break between P5 and M1 leaves development of the cingula in the distal premolars a less-convincing criterion. One final possibility is that P4 is the distal premolar and P5 is the first molar. Other than some minor differences in cingular cusps, these two teeth are quite similar to one another and no sharp morphological break can be identified between them. Comparative aspects of wear are more complicated but equivocal, with the P4 showing more distal wear (especially on the metacone) and P5 showing a much more heavily excavated B cusp. Both of these teeth are still less worn than the M1, supporting our original interpretation that they represent premolars.

Comparisons.—The shape and proportions of the preserved skull elements of *Cifellilestes ciscoensis* gen. et sp. nov. are quite similar to those of *Morganucodon* spp. (Kermack et al. 1981; Luo et al. 1995). One prominent difference is the number of infraorbital foramina: in *Morganucodon watsoni* there are three openings for branches of the infraorbital neurovasculature, and this is reflected also by separate grooves in the canal itself (Kermack et al. 1981: fig. 13). *Morganucodon oehleri* has at least two infraorbital foramina (Luo et al. 1995). There is only one large groove for the infraorbital canal and a single large opening on the facial process of the maxilla in *Cifellilestes ciscoensis* (Figs. 1, 2, 4). *Cifellilestes ciscoensis* gen. et sp. nov. also has a distinct buccinator ridge contouring along the base of the snout, just dorsal to the alveoli (Fig. 1A$_1$). *Morganucodon* spp. lack evidence of this feature (Kermack et al. 1981; Luo et al. 1995), suggesting fleshy cheeks were present in *C. ciscoensis* and were at least better developed than in *Morganucodon* spp. (Hahn 1985; Muchlinski 2008; Benoit et al. 2016a). The facial process of the maxilla is much taller in *C. ciscoensis* and the infraorbital foramen positioned proportionately more dorsally than in *Morganucodon* spp.; the snout in *C. ciscoensis* would have been somewhat more rectangular in coronal section than in *Morganucodon* spp. The posterior extent of the bony palate also differs between these taxa, reaching the front of the last molar in *C. ciscoensis* while in *Morganucodon* spp. it extends to the rear of the tooth row; additionally, the opening of the greater palatine foramen is more posteriorly positioned in *Morganucodon* spp., at the level of the 6th postcanine tooth (M2 in that taxon) as opposed to the P4 in *C. ciscoensis*. The thick pterygoid process of the palatine in *C. ciscoensis* more closely resembles the condition in *Brasilitherium riograndensis* Bonaparte, Martinelli, Schultz, and Rupert, 2003 (= *Brasilodon*) than in *Morganucodon* spp. (Ruf et al. 2014), though in the latter this structure is less well preserved.

The postcanine dental formula differs between *C. ciscoensis* and species of *Morganucodon*, particularly with regard to the lower number of molars in the new taxon. The largest upper molar in both taxa is also the position of strong imbrication of the tooth row, M1 in *C. ciscoensis* and M2 in *Mo. watsoni* (Fig. 6). The deepest palatal pit, indicating the position of the largest lower tooth, is found mesial to this tooth position in both taxa. The next distal molar in both taxa is similarly imbricated but substantially smaller; an additional small molar is present in *Mo. watsoni*, but this position is lost in *C. ciscoensis*. If this peg-like, single-rooted ultimate molar in *Mo. watsoni* is disregarded, both *C. ciscoensis* and *Mo. watsoni* have seven postcanine teeth suggesting a degree of underlying homology. The mechanism at work modifying tooth replacement (and therefore the molar and premolar counts) in morganucodontans may have resulted in a fluid premolar–molar boundary within this group, making differences in molar or premolar count somewhat less meaningful especially when the total postcanine count is the same. It appears likely that the M1

and M2 tooth positions in *C. ciscoensis* are homologous with the M2 and M3 positions in *Mo. watsoni*; this, coupled with the presence of an additional premolar in *C. ciscoensis* (P5), suggests that the premolar–molar boundary migrated one position distally relative to *Mo. watsoni* in the line leading to *C. ciscoensis* (or, potentially, retention of a primitive pattern of replacement in *C. ciscoensis*). However, substantial differences remain between the premolars of these taxa. The anterior premolars in *Mo. watsoni* are small, simple, and single-rooted, with the last premolar (P4) departing significantly in size and shape: while still premolariform, it is double-rooted and very large (Kermack et al. 1981; Jäger et al. 2019; Fig. 6). There is no correlate for this pattern in the premolars in *C. ciscoensis*: all are double rooted and increase gradually in size and complexity, with the P4 and P5 largest and most molariform. *Morganucodon oehleri* more closely resembles *C. ciscoensis* in general proportions of the premolar series (Crompton and Luo 1993; but see differences in Luo et al. 1995), though these teeth lack the strong molarization seen in *C. ciscoensis*. The P5 of *C. ciscoensis* and M1 of *Mo. watsoni* are similar in relative size and in orientation (lack of imbrication), but the cusp proportions and spacing are different. Differences exist in molarization of the premolars and relative morphology of the crowns straddling the premolar–molar boundary in these taxa, and the premolars are more similar to what we see in eutriconodontans, with well developed metacones and tall centrally placed paracones. Simply shifting the point of transition cannot fully explain the story.

While tooth formula in *C. ciscoensis* also differs from that described in *Mo. oehleri* (Luo et al. 1995), these taxa could be congruent if *Mo. oehleri* is reinterpreted. The tooth identified as M1 in *Mo. oehleri* has a complete complement of cingula but a very tall central cusp with much lower flanking cusps (Luo et al. 1995: fig. 4), resembling the P4 or P5 of *C. ciscoensis*. The next distal tooth has main cusps that are much less disparate in height, resembling the molars in *Mo. watsoni* and *C. ciscoensis*. As postulated here, the presence of complete lingual and buccal cingula need not be defining characteristics of molars; based on cusp proportions, the M1 of *Mo. oehleri* more closely resembles a distal premolar. Under this interpretation, the postcanine formula in this taxon would be P5–M2, as in *C. ciscoensis*.

The shift in cusp proportions at the premolar–molar transition in *C. ciscoensis* also resembles that described for the Early Jurassic morganucodontan *Megazostrodon rudnerae* Crompton and Jenkins, 1968, from southern Africa (Crompton 1974; Gow 1986). This taxon has five premolars and four to five molars (Gow 1986; Jäger et al. 2019); the ultimate premolar is tall but remains premolariform, with a dominant paracone and much smaller flanking cusps. The M1 is much lower crowned with a paracone only slightly taller than the other main cusps. *Dinnetherium nezorum* Jenkins, Crompton, and Downs, 1983, from the Lower Jurassic Kayenta Formation of Arizona (USA), has been considered closely related to *Megazostrodon rudnerae* and

is known by a nearly complete postcanine dentition (Jenkins et al. 1983; Gow 1986; Rougier et al. 2012). Nine postcanine teeth are present in the lower jaws, and while five upper molars are described the number of upper premolars is uncertain. The upper molar cusp proportions in *D. nezorum* differ somewhat from *Me. rudnerae* and *C. ciscoensis* in that the paracone is substantially taller than cusp B and the metacone on all but the ultimate molar. While it is possible that some mesial molar positions in *D. nezorum* could represent premolars, caution is warranted until the entire upper postcanine dentition is better preserved as expansion of the premolar count beyond five is very unlikely (described only in the Early Cretaceous australosphenidan *Bishops whitmorei* Rich, Flannery, Trusler, Kool, Klavern, and Vickers-Rich, 2001). *Cifellilestes ciscoensis* gen. et sp. nov. differs from both *Me. rudnerae* and *D. nezorum* in having a strong imbrication of the molars relative to the premolar row (Fig. 6).

Cifellilestes ciscoensis gen. et sp. nov. compares favorably in overall proportions with *Bridetherium dorisae* Clemens, 2011, from the Early Jurassic of Wales (Clemens 2011), but differs in the larger size of the metastyle and in the size and proportions of the buccal cingulum and cingular cusps. Unfortunately, *B. dorisae* is known only by isolated molars. *Storchodon cingulatus* Martin, Averianov, Jäger, Schwermann, Oliver, and Wings, 2019, known by a single upper molar from the Late Jurassic of Germany (Martin et al. 2019), shares with *C. ciscoensis* a large, somewhat buccally-displaced metastyle but differs in a much larger overall crown size and in the relative proportions of the paracone and metacone (the latter being a much larger cusp than in *C. ciscoensis*).

Butler et al. (2012) described a morganucodontan from the Lower Cretaceous Lulworth Formation (Purbeck Group), southern England. The isolated teeth referred to *Purbeckodon batei* Butler, Sigogneau-Russell, and Ensom, 2011 (identified as molars) are all distinctly low-crowned but have a strongly asymmetrical main cusp with very small flanking cusps. Cingula on the upper teeth are well developed and cuspidate but the buccal cingula are incomplete. This taxon is likely a morganucodontan, but these specimens most closely resemble premolars from the middle of the series (Fig. 6). While this is the youngest record for the group anywhere in the world, the Morrison Formation and Purbeck Group are close in age and their faunas have historically been compared (e.g., Osborn 1897; Simpson 1928, 1929; Butler 1939). However, we are hesitant to place much weight in comparisons between *C. ciscoensis* and *P. batei* until the latter is represented by molars.

Though not identified as a morgancodontan, the small mammaliaform *Hadrocodium wui* Luo, Crompton, and Sun, 2001, from the Early Jurassic of China (Luo et al. 2001) is relevant to this discussion. This taxon is known by a skull of an adult individual and has only two upper molars, a feature it shares with *C. ciscoensis*. However, *H. wui* has just three premolars and the upper molars lack the complete, cuspidate cingula characteristic of morganucodontans.
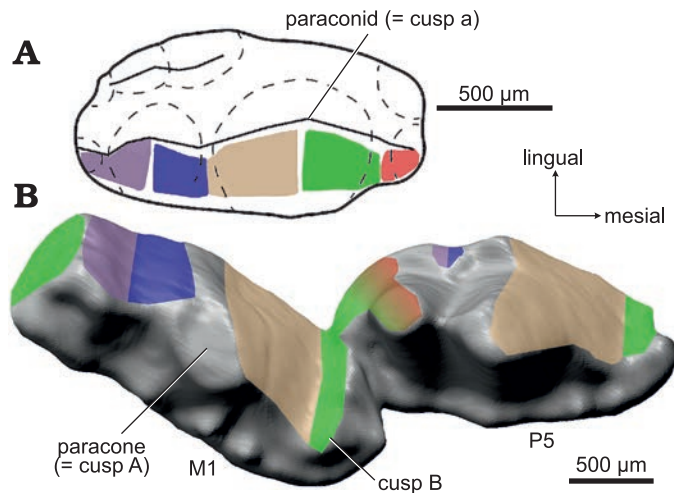
Fig. 7. Hypothetical molar occlusal wear facet pattern in P5–M1 of *Cifellilestes ciscoensis* gen. et sp. nov. (**B**, OMNH 69352), with illustration of a lower molar modified from *Morganucodon watsoni* Kühne, 1949 (**A**, m2, UMZC_Eo.CR.1, reversed). Corresponding colors on upper and lower teeth indicate matching wear facets. The occlusal pattern of *C. ciscoensis* is similar to *M. watsoni* in that the protoconid (also referred to as cusp a) of the lower molars occludes between the upper molar paracone (also referred to as cusp A) and cusp B, carving a prominent groove between the two cusps. This also results in contact to the next mesial tooth, due to the size of the protoconid. The paracone occludes between the protoconid and metaconid (also referred to as cusp c). Modified after Jäger et al. (2019).

Analysis of molar occlusion.—Minor apical wear is present in *Cifellilestes ciscoensis* gen. et sp. nov. in P1–P3 (Fig. 1B). The P3 additionally has an incipient facet on the distolingual cingulum, caused by contact of the protoconid of the lower p4. This contact is continued onto the mesiolingual side of P4 with a large facet on the anterior flank of cusp B. A second facet, caused by the protoconid of p5, encompasses the distolingual cingulum and flanks of the metacone and metastyle.

P5 is more worn than P4. A prominent groove is present between cusp B and the paracone, indicating that the protoconid of p5 occluded slightly more posterior than that of p4. The distolingual facet in P5 is smaller than that of P4, as it is limited to the distal-most portion of the cingulum and cusp D. Wear in the last two premolars correlates with the placement of the maxillary pits and the occlusal pattern is similar to that of molars in *Morganucodon* spp. (Crompton and Jenkins 1968; Mills 1971; Jäger et al. 2019) (Figs. 1A₃, 4A₃, 7).

The occlusal pattern resembles that of *Morganucodon watsoni*, with the lower molar protoconid occluding in between upper molar cusp B and the paracone and the upper molar paracone occluding between the lower molar protoconid and metaconid (Fig. 7). Apart from *Mo. watsoni*, this pattern is otherwise only known from *Storchodon cingulatus* and potentially *Dinnetherium nezorum* (Crompton and Luo 1993; Martin et al. 2019). It differs from *Bridetherium dorisae* where wear is primarily present directly on the lingual side of the cusps, rather than in the valleys between (Clemens 2011).

Embrasure occlusion, where the lower molar protoconid occludes in the space between two opposing upper molars, is commonly found in morganucodontans (e.g.,

Megazostrodon rudnerae and *Erythrotherium parringtoni* Crompton, 1964, see Crompton 1974; Jäger et al. 2019) but can be excluded based on the prominent grooves between cusps B and the paracone, as well as the prominent wear between the paracone and metacone (Fig. 7). Despite differences between *C. ciscoensis* and *Morganucodon watsoni* regarding upper molar proportions and premolar cingula, the similarity in the occlusal pattern between these taxa suggests that the lower molars and posterior premolars of *C. ciscoensis* were likely morphologically similar to those of *Mo. watsoni*. One possible difference might be that the lower molars of *C. ciscoensis* possessed a taller but slightly more slender protoconid relative to *Mo. watsoni*, based on the depth of the maxillary pits and the reduced amount of wear on the distal side of each molar in the new taxon.

Conclusions

Morganucodontans were abundant components of Early Jurassic small vertebrate faunas worldwide, and the group illustrates the plesiomorphic pattern characterizing the milieu from which mammals arose. Records of this group surviving later in the Jurassic are quite rare: *Cifellilestes ciscoensis* gen. et sp. nov. is the first morganucondontan known from the Upper Jurassic Morrison Formation (a unit in the western USA that has received intense focus for nearly 150 years), and other members of this group have been recovered from somewhat coeval units in Great Britain and Germany (Butler et al. 2012; Martin et al. 2019). In contrast docodontans, another mammaliaform lineage, are common across most Morrison Formation localities (though so far conspicuously absent from others, including FPA and CMQ, Foster et al. 2006). The presence of the distinctive and highly specialized *Fruitafossor windscheffeli* in only FPA and CMQ (Luo and Wible 2005; Davis et al. 2018; BMD unpublished data), in addition to other new taxa from the CMQ currently under study, suggests that diversity from the Morrison Formation is not yet fully realized. The estimated age range of the CMQ overlaps with that of the FPA, and lithology and many aspects of the known fauna are also quite similar. This new locality does not appear close to exhausted, and we expect that future discoveries will not only augment what is known from the FPA but hopefully provide additional morphological data for *C. ciscoensis*.

While this new record extends the tenure of morganucodontans on the North American landmass by more than 30 Ma, dispersal of terrestrial vertebrates during the Jurassic was relatively unimpeded even as the Atlantic was beginning to open at the end of the Period (Kocsis and Scotese 2021); though rare, morganucodontan-like teeth are known from the Late Jurassic of Germany and the earliest Cretaceous of Great Britain (Butler et al. 2012; Martin et al. 2019). The discovery of *C. ciscoensis* has less of an impact on our understanding of the temporospatial distribution of morganucodontans, if these taxa indeed form a

monophyletic group, than it does on uncovering patterns of craniodental evolution in a group anchored at the base of Mammaliaformes yet diversifying through at least the entirety of the Jurassic. Our new taxon demonstrates a novel postcanine tooth formula for the group and greater molarization of premolars, possibly suggesting modification of the ontogenetic processes governing the premolar–molar boundary (or, alternatively, retention of a primitive pattern). The presence in *C. ciscoensis* of a more sophisticated pattern of innervation to the snout (via a single large infraorbital foramen) and of fleshy cheeks (suggested by the presence of a buccinator ridge) suggests that this record is not simply one of a lone survivor of an ancient lineage, but instead demonstrates that complex character systems (beyond rearrangements of cusps on molars) were undergoing modification in morganucodontan evolution.

Acknowledgements

References

Benoit, J., Abdala, F., Manger, P.R., and Rubidge, B. 2016a. The sixth sense in mammalian forerunners: Variability of the parietal foramen and the evolution of the pineal eye in South African Permo-Triassic eutheriodont therapsids. *Acta Palaeontologica Polonica* 61: 777–789.

Benoit, J., Manger, P.R., and Rubidge, B.S. 2016b. Palaeoneurological clues to the evolution of defining mammalian soft tissue traits. *Scientific Reports* 6: 25604.

Benoit, J., Ruf, I., Miyamae, J.A., Fernandez, V., Rodrigues, P.G., and Rubidge, B.S. 2020. The evolution of the maxillary canal in Probainognathia (Cynodontia, Synapsida): reassessment of the homology of the infraorbital foramen in mammalian ancestors. *Journal of Mammalian Evolution* 27: 329–348.

Bi, S., Zheng, X., Meng, J., Wang, X., Robinson, N., and Davis, B. 2016. A new symmetrodont mammal (Trechnotheria: Zhangheotheriidae) from the Early Cretaceous of China and trechnotherian character evolution. *Scientific Reports* 6: 26668.

Bonaparte, J.F. 1980. El primer ictidosaurio (Reptilia–Therapsida) de América del Sur, Chalminia musteloides, del Tríasico Superior del La Rioja, República Argentina. *Actas del II Congreso Argentino del Paleontología y Bioestratigrafía, y I Congreso Latinamericano de Paleontología* 1: 123–133.

Bonaparte, J.F., Martinelli, A.G., Schultz, C.L., and Rubert, R. 2003. The sister group of mammals: small cynodonts from the Late Triassic of southern Brazil. *Revista Brasileira de Paleontologia* 5: 2–27.

Brinkkötter, J.J. 2019. *Molar Dentition of the Docodontan Haldanodon (Mammaliaformes) as Functional Analog to Tribosphenic Teeth*. 169 pp. Rheinische Friedrich-Wilhelms-Universität, Bonn.

Butler, P.M. 1939. The teeth of the Jurassic mammals. *Proceedings of the Zoological Society of London* 109: 329–356.

Butler, P.M. 1997. An alternative hypothesis on the origin of docodont molar teeth. *Journal of Vertebrate Paleontology* 17: 435–439.

Butler, P.M. and Sigogneau-Russell, D. 2016. Diversity of triconodonts in the Middle Jurassic of Great Britain. *Palaeontologia Polonica* 67: 35–65.

Butler, P.M., Sigogneau-Russell, D., and Ensom, P.C. 2012. Possible persistence of the morganucodontans in the Lower Cretaceous Purbeck Limestone Group (Dorset, England). *Cretaceous Research* 33: 135–145.

Callison, G. 1987. Fruita: a place for wee fossils. *In*: W.R. Averett (ed.), *Paleontology and Geology of the Dinosaur Triangle*, 91–96. Museum of Western Colorado, Grand Junction.

Clemens, W.A. 2011. New morganucodontans from an Early Jurassic fissure filling in Wales (United Kingdom). *Palaeontology* 54: 1139–1156.

Crompton, A.W. 1974. The dentition and relationships of the southern African Triassic mammals, *Erythrotherium parringtoni* and *Megazostrodon rudnerae*. *Bulletin of the British Museum (Natural History), Geology* 24: 397–437.

Crompton, A.W. and Jenkins, F.A., Jr. 1968. Molar occlusion in Late Triassic mammals. *Biological Reviews* 43: 427–458.

Crompton, A.W. and Luo, Z.-X. 1993. Relationships of the Liassic mammals *Sinoconodon*, *Morganucodon*, and *Dinnetherium*. *In*: F.S. Szalay, M.J. Novacek, and M.C. McKenna (eds.), *Mammal Phylogeny, Volume 2. Mesozoic Differentiation, Multituberculates, Monotremes, Early Therians, and Marsupials*, 30–44. Springer-Verlag, Inc., New York.

Crompton, A.W., Owerkowicz, T., Bhullar, B.A.S., and Musinsky, C. 2017. Structure of the nasal region of non-mammalian cynodonts and mammaliaforms: Speculations on the evolution of mammalian endothermy. *Journal of Vertebrate Paleontology* 37 (1): e1269116.

Davis, B.M. 2011. A novel interpretation of the tribosphenidan mammal *Slaughteria eruptens* from the Early Cretaceous Trinity Group, and implications for dental formula in early mammals. *Journal of Vertebrate Paleontology* 31: 676–683.

Davis, B.M., Cifelli, R.L., and Rougier, G.W. 2018. A preliminary report of the fossil mammals from a new microvertebrate locality in the Upper Jurassic Morrison Formation, Grand County, Utah. *Geology of the Intermountain West* 5 (1): 1–8.

Davis, B.M., Cifelli, R.L., and Rougier, G.W. 2021. Mammalian petrosals from the Upper Jurassic Morrison Formation (Utah, USA) reveal non-canonical middle and inner ear character evolution. *Journal of Mammalian Evolution* 28: 1027–1049.

Debuysschere, M., Gheerbrant, E., and Allain, R. 2015. Earliest known European mammals: a review of the Morganucodonta from Saint-Nicolas-de-Port (Upper Triassic, France). *Journal of Systematic Palaeontology* 13: 825–855.

Doelling, H.H. 2002. *Geologic Map of the Moab and Eastern Part of the San Rafael Desert 30'x60'Quadrangles, Grand and Emery Counties, Utah, and Mesa County, Colorado. Utah Geological Survey Geologic Map 180*. Utah Geological Survey, Salt Lake City.

Engelmann, G.F. and Callison, G. 1998. Mammalian faunas of the Morrison Formation. *Modern Geology* 23: 343–379.

Engelmann, G.F. and Callison, G. 1999. *Glirodon grandis*, a new multituberculate mammal from the Upper Jurassic Morrison Formation. *In*: D.D. Gillette (ed.), Vertebrate Paleontology in Utah. *Utah Geological Survey Special Publication* 99-1: 161–177.

Foster, J.R., Trujillo, K., and Chamberlain, K. 2017. A preliminary U-Pb zircon age for the Fruita Paleontological Area microvertebrate localities, Upper Jurassic Morrison Formation, Mesa County, CO. *Journal of Vertebrate Paleontology, Program and Abstracts* 2017: 113.

Foster, J.R., Trujillo, K.C., Madsen, S.K., and Martin, J.E. 2006. The Late Jurassic mammal *Docodon*, from the Morrison Formation of the Black Hills, Wyoming: implications for abundance and biogeography of the genus. *New Mexcio Museum of Natural History and Science Bulletin* 36: 165–169.

Freeman, E.F. 1979. A Middle Jurassic mammal bed from Oxfordshire. *Palaeontology* 22: 135–166.

Gaetano, L. and Rougier, G. 2012. First amphilestid from South America: a molariform from the Jurassic Cañadón Asfalto Formation, Patagonia, Argentina. *Journal of Mammalian Evolution* 19: 235–248.

Gow, C.E. 1986. A new skull of *Megazostrodon* (Mammalia: Triconodonta) from the Elliot Formation (Lower Jurassic) of southern Africa. *Palaeontologia Africana* 26: 13–23.

Hahn, G. 1985. Zum Bau des Infraorbital-Foramens bei den Paulchoffatiidae (Multituberculata, Ober-Jura). *Berliner Geowissenschaftliche Abhandlungen A* 60: 5–27.

Harper, T. and Rougier, G.W. 2019. Petrosal morphology and cochlear function in Mesozoic stem therians. *PLOS ONE* 14 (8): e0209457.

Jäger, K.R.K., Cifelli, R.L., and Martin, T. 2020. Molar occlusion and jaw roll in early crown mammals. *Scientific Reports* 10 (1): 22378.

Jäger, K.R.K., Gill, P.G., Corfe, I., and Martin, T. 2019. Occlusion and dental function of *Morganucodon* and *Megazostrodon*. *Journal of Vertebrate Paleontology* 39 (3): e1635135.

Jenkins, F.A., Jr. and Schaff, C.R. 1988. The Early Cretaceous mammal *Gobiconodon* (Mammalia, Triconodonta) from the Cloverly Formation in Montana. *Journal of Vertebrate Paleontology* 8: 1–24.

Jenkins, F.A., Jr., Crompton, A.W., and Downs, W.R. 1983. Mesozoic mammals from Arizona: new evidence on mammalian evolution. *Science* 222: 1233–1235.

Kermack, K.A., Mussett, F., and Rigney, H.W. 1973. The lower jaw of *Morganucodon*. *Journal of the Linnean Society (Zoology)* 53: 87–175.

Kermack, K.A., Mussett, F., and Rigney, H.W. 1981. The skull of *Morganucodon*. *Zoological Journal of the Linnean Society* 71: 1–158.

Kielan-Jaworowska, Z., Cifelli, R.L., and Luo, Z.-X. 2004. *Mammals from the Age of Dinosaurs: Origins, Evolution, and Structure*. 700 pp. Columbia University Press, New York.

Kirkland, J.I. 2006. Fruita Paleontological Area (Upper Jurassic, Morrison Formation), western Colorado: an example of terrestrial taphofacies analysis. *New Mexico Museum of Natural History and Science Bulletin* 36: 67–95.

Kirkland, J.I., Suarez, M., Suarez, C., and Hunt-Foster, R. 2017. The Lower Cretaceous in east-central Utah—the Cedar Mountain Formation and its bounding strata. *Geology of the Intermountain West* 3: 101–228.

Kocsis, Á.T. and Scotese, C.R. 2021. Mapping paleocoastlines and continental flooding during the Phanerozoic. *Earth-Science Reviews* 213: 103463.

Kühne, W.G. 1949. On a triconodont tooth of a new pattern from a fissure-filling in South Glamorgan. *Proceedings of the Zoological Society of London* 119: 345–350.

Kühne, W.G. and Krusat, G. 1972. Legalisierung des taxon Haldanodon (Mammalia, Docodonta). *Neues Jahrbuch für Geologie, Paläontologie und Mineralogie, Monatshefte* 5: 300–302.

Lillegraven, J.A. and Krusat, G. 1991. Cranio-mandibular anatomy of *Haldanodon exspectatus* (Docodonta; Mammalia) from the Late Jurassic of Portugal and its implications to the evolution of mammalian characters. *Contributions to Geology, University of Wyoming* 28 (2): 39–138.

Lopatin, A. and Averianov, A. 2015. *Gobiconodon* (Mammalia) from the Early Cretaceous of Mongolia and Revision of Gobiconodontidae. *Journal of Mammalian Evolution* 22: 17–43.

Lopatin, A.V., Averianov, A.O., Maschenko, E.N., and Leshchinskiy, S.V. 2010. Early Cretaceous mammals of Western Siberia: 3. Zhangheotheriidae. *Paleontological Journal* 44: 573–583.

Luckett, W.P. 1993. An ontogenetic assessment of dental homologies in therian mammals. *In*: F.S. Szalay, M.J. Novacek, and M.C. McKenna (eds.), *Mammal Phylogeny, Volume 2. Mesozoic Differentiation, Multituberculates, Monotremes, Early Therians, and Marsupials*, 182–204. Springer-Verlag, New York.

Luo, Z.-X. 2011. Developmental patterns in Mesozoic evolution of mammal ears. *Annual Review of Ecology, Evolution, and Systematics* 42: 355–380.

Luo, Z.-X. and Wible, J.R. 2005. A Late Jurassic digging mammal and early mammalian diversification. *Science* 308: 103–107.

Luo, Z.-X., Crompton, A.W., and Sun, A.-L. 2001. A new mammaliaform from the Early Jurassic and evolution of mammalian characteristics. *Science* 292: 1535–1540.

Luo, Z.-X., Kielan-Jaworowska, Z., and Cifelli, R.L. 2004. Evolution of dental replacement in mammals. *Bulletin of the Carnegie Museum of Natural History* 36: 159–175.

Luo, Z.-X., Lucas, S.G., Li, J.-L., and Zhen, S. 1995. A new specimen of *Morganucodon oehleri* (Mammalia, Triconodonta) from the Liassic Lufeng Formation of Yunnan, China. *Neues Jahrbuch für Geologie und Paläontologie Monatschefte* 11: 671–680.

Maidment, S.C.R. and Muxworthy, A. 2019. A chronostratigraphic framework for the Upper Jurassic Morrison Formation, western U.S.A. *Journal of Sedimentary Research* 89: 1017–1038.

Maier, W. 1993. Cranial morphology of the therian common ancestor, as suggested by the adaptations of neonate marsupials. *In*: F.S. Szalay, M.J. Novacek, and M.C. McKenna (eds.), *Mammal Phylogeny: Mesozoic Differentiation, Multituberculates, Monotremes, Early Therians, and Marsupials*, 165–181. Springer-Verlag, New York.

Marsh, O.C. 1878. Fossil mammal from the Jurassic of the Rocky Mountains. *American Journal of Science* 15: 459.

Martin, T., Averianov, A., Jäger, K.R.K., Schwermann, A.H., and Wings, O. 2019. A large morganucodontan mammaliaform from the Late Jurassic of Germany. *Fossil Imprint* 75: 504–509.

Martinelli, A.G. and Rougier, G.W. 2007. On *Chaliminia musteloides* (Eucynodontia: Tritheledontidae) from the Late Triassic of Argentina, and a phylogeny of Ictidosauria. *Journal of Vertebrate Paleontology* 27: 442–460.

Martinelli, A.G., Eltink, E., Da-Rosa, Á.A.S., and Langer, M.C. 2017. A new cynodont from the Santa Maria formation, south Brazil, improves Late Triassic probainognathian diversity. *Papers in Palaeontology* 3: 401–423.

Martinelli, A.G., Soto-Acuña, S., Goin, F.J., Kaluza, J., Bostelmann, J.E., Fonseca, P.H.M., Reguero, M.A., Leppe, M., and Vargas, A.O. 2021. New cladotherian mammal from southern Chile and the evolution of mesungulatid meridiolestidans at the dusk of the Mesozoic era. *Scientific Reports* 11 (1): 7594.

McKenna, M.C. 1975. Toward a phylogenetic classification of the Mammalia. *In*: W.P. Luckett, and F.S. Szalay (eds.), *Phylogeny of the Primates*, 21–46. Plenum Press, New York.

Mills, J.R.E. 1971. The dentition of *Morganucodon*. *In*: D.M. Kermack and K.A. Kermack (eds.), Early Mammals. *Zoological Journal of the Linnean Society* 50: 29–63.

Muchlinski, M.N. 2008. The relationship between the infraorbital foramen, infraorbital nerve, and maxillary mechanoreception: Implications for interpreting the paleoecology of fossil mammals based on infraorbital foramen size. *The Anatomical Record* 291: 1221–1226.

O'Meara, R.N., Dirks, W., and Martinelli, A.G. 2018. Enamel formation and growth in non-mammalian cynodonts. *Royal Society Open Science* 5 (5): 172293.

Osborn, H.F. 1888. Additional observations upon the structure and classification of the Mesozoic Mammalia. *Proceedings of the Academy of Natural Sciences, Philadelphia* 1888: 292–301.

Osborn, H.F. 1897. Trituberculy: a review dedicated to the late Professor Cope. *American Naturalist* 31: 993–1016.

Owen, R. 1868. *On the Anatomy of Vertebrates. Vol. 3. Mammals*. 915 pp. Longmans, Greens and Co., London.

Parrington, F.R. 1978. A further account of the Triassic mammals. *Philosophical Transactions of the Royal Society of London B* 282: 177–204.

Patterson, B. 1956. Early Cretaceous mammals and the evolution of mammalian molar teeth. *Fieldiana: Geology* 13: 1–105.

Pietrokovski, J. and Massler, M. 1967. Ridge remodeling after tooth extraction in rats. *Journal of Dental Research* 46: 222–231.

Prothero, D.R. 1981. New Jurassic mammals from Como Bluff, Wyoming, and the interrelationships of non-tribosphenic Theria. *Bulletin of the American Museum of Natural History* 167: 277–326.

Rasmussen, T.E. and Callison, G. 1981. A new species of triconodont mammal from the Upper Jurassic of Colorado. *Journal of Paleontology* 55: 628–634.

Rich, T.H., Flannery, T.F., Trusler, P., Kool, L., van Klaveren, N., and Vickers-Rich, P. 2001. A second tribosphenic mammal from the Mesozoic of Australia. *The Records of the Queen Victoria Museum* 110: 1–9.

Rigney, H.W. 1963. A specimen of *Morganucodon* from Yunnan. *Nature* 197: 1122–1123.

Rougier, G.W., Garrido, A., Gaetano, L., Puerta, P., Corbitt, C., and Novacek, M.J. 2007a. First Jurassic triconodont from South America. *American Museum Novitates* 3850: 1–17.

Rougier, G.W., Isaji, S., and Manabe, M. 2007b. An Early Cretaceous mammal from the Kuwajima Formation (Tetori Group), Japan, and a reassessment of triconodont phylogeny. *Annals of the Carnegie Museum* 76: 73–115.

Rougier, G.W., Ji, Q., and Novacek, M.J. 2003a. A new symmetrodont mammal with fur impressions from the Mesozoic of China. *Acta Geologica Sinica* 77: 7–14.

Rougier, G.W., Sheth, A.S., Carpenter, K., Appella-Guiscafre, L., and Davis, B.M. 2014. A new species of *Docodon* (Mammaliaformes: Docodonta) from the Upper Jurassic Morrison Formation and a reassessment of selected craniodental characters in basal mammaliaforms. *Journal of Mammalian Evolution* 22: 1–16.

Rougier, G.W., Spurlin, B.K., and Kik, P.K. 2003b. A new specimen of *Eurylambda aequicrurius* and considerations on "symmetrodont" dentition and relationships. *American Museum Novitates* 3394: 1–15.

Rougier, G.W., Wible, J.R., and Hopson, J.A. 1996. Basicranial anatomy of *Priacodon fruitaensis* (Triconodontidae, Mammalia) from the Late Jurassic of Colorado, and a reappraisal of mammaliaform interrelationships. *American Museum Novitates* 3183: 1–38.

Rougier, G.W., Wible, J.R., Beck, R., and Apesteguía, S. 2012. The Miocene mammal *Necrolestes* demonstrates the survival of a Mesozoic non-therian lineage into the late Cenozoic of South America. *Proceedings of the National Academy of Sciences* 109: 20053–20058.

Rowe, T.B. 1988. Definition, diagnosis, and origin of Mammalia. *Journal of Vertebrate Paleontology* 8: 241–264.

Rowe, T.B. 1993. Phylogenetic systematics and the early history of mammals. *In*: F.S. Szalay, M.J. Novacek, and M.C. McKenna (eds.), *Mammal Phylogeny, Volume 2: Mesozoic Differentiation, Multituberculates, Monotremes, Early Therians, and Marsupials*, 129–145. Springer-Verlag, New York.

Rowe, T.B. and Shepherd, G.M. 2016. Role of ortho-retronasal olfaction in mammalian cortical evolution. *Journal of Comparative Neurology* 524 (3): 471–495.

Ruf, I., Maier, W., Rodrigues, P.G., and Schultz, C.L. 2014. Nasal anatomy of the non-mammaliaform cynodont *Brasilitherium riograndensis* (Eucynodontia, Therapsida) reveals new insight into mammalian evolution. *The Anatomical Record* 297: 2018–2030.

Simpson, G.G. 1928. *A Catalogue of the Mesozoic Mammalia in the Geological Department of the British Museum*. 215 pp. Trustees of the British Museum, London.

Simpson, G.G. 1929. American Mesozoic Mammalia. *Memoirs of the Peabody Museum* 3 (1): 1–235.

Slaughter, B.H. 1981. The Trinity therians (Albian, mid-Cretaceous) as marsupials and placentals. *Journal of Paleontology* 55: 682–683.

Trujillo, K., Carrano, M., and Chamberlain, K. 2015. A U-Pb zircon age for Reed's Quarry 9, Upper Jurassic Morrison Formation, Albany County, WY. *Journal of Vertebrate Paleontology,* Programs and Abstracts 2015: 226.

Trujillo, K.C. and Kowallis, B. 2015. Recalibrated ^{40}Ar/^{39}Ar ages for the Upper Jurassic Morrison Formation, Western Interior, U.S.A. *Geology of the Intermountain West* 2: 1–8.

Turner, C.E. and Peterson, F. 2004. Reconstruction of the Upper Jurassic Morrison Formation extinct ecosystem—a synthesis. *Sedimentary Geology* 167: 309–355.

Wible, J.R. and Hopson, J.A. 1993. Basicranial evidence for early mammal phylogeny. *In*: F.S. Szalay, M.J. Novacek, and M.C. McKenna (eds.), *Mammal Phylogeny, Volume 1: Mesozoic Differentiation, Multituberculates, Monotremes, Early Therians, and Marsupials*, 45–62. Springer-Verlag, New York.